

**Figure 7.** (a) Ratio of the  $E(2\omega)$  measured before and after illumination by a single pulse of intensity  $I$ . (b) Dynamics of photodesorption.  $I(\text{pump}) = 300 \text{ mJ}/\text{cm}^2$ .

#### IV. Conclusions

The technique of time-resolved surface second harmonic generation has been studied. The method yields a surface-specific signal which has been used to study the excited-state dynamics

of adsorbates at submonolayer coverages. The similarities and differences of this nonlinear optical method to linear methods, such as time-resolved fluorescence and transient absorption, have been described. A comparison of the TRF and TRSSHG data showed that the latter technique reliably reports the adsorbate dynamics provided that the proper power levels are employed.

Three different dye molecules adsorbed on optically flat silica plates were studied. It was observed that intramolecular motion (excited-state isomerization) can occur on a picosecond time scale in adsorbed molecules. The adsorbate spectra and isomerization dynamics were contrasted with the behavior of the same molecules in solution. In no case was there a precise analogy. Rather, the details of the adsorbate-substrate interaction dominate the observed isomerization dynamics. Two limiting cases have been described. The dynamics of a multiphoton photodesorption were also studied. The rate was faster than the current time resolution, but the mechanism has not been determined.

The present results indicate that second-order nonlinear optical effects will be a reliable and moderately sensitive method for the study of surface reaction kinetics in the condensed phase on a picosecond time scale. Such data will add an important new dimension to studies in surface science, catalysis, and surface laser chemistry. Recently the method was extended to the solid-liquid interface, using a total internal reflection geometry.<sup>47</sup>

**Acknowledgment.** We are grateful to Dr. Klaus Kemnitz for a careful measurement of the fluorescence decays and to Dr. Hrvoje Petek for a critical reading of the manuscript. S.R.M. gratefully acknowledges financial support from the Inoue Science Foundation, the Science and Engineering Research Council, the Royal Society, and the British Council at various stages of the project, and Heriot-Watt University for leave of absence.

(47) Meech, S. R.; Yoshihara, K. Manuscript in preparation.

## Resonance Raman Spectra of 13-Demethylretinal Bacteriorhodopsin and of a Picosecond Bathochromic Photocycle Intermediate

T. Noguchi,<sup>†</sup> S. Kolaczowski,<sup>†</sup> W. Gärtner,<sup>\*,‡</sup> and G. H. Atkinson<sup>\*,†,§</sup>

Department of Chemistry and Optical Science Center, University of Arizona, Tucson, Arizona 85721, and Institut für Biologie I, University of Freiburg, D-7800 Freiburg, Federal Republic of Germany  
(Received: October 17, 1989)

Resonance Raman spectra of an artificial bacteriorhodopsin pigment containing a 13-demethylretinal chromophore and of a bathochromic photocycle intermediate formed within 150 ps are presented. The frequency shifts observed in spectra recorded from samples in  $\text{H}_2\text{O}$  and  $\text{D}_2\text{O}$  solvents yield vibrational assignments which identify the 13-demethyl pigment as containing a  $\text{C}_{13}=\text{C}_{14}$  cis,  $\text{C}_{15}=\text{N}$  syn configuration of retinal and a bathochromic intermediate at 150 ps as containing the  $\text{C}_{13}=\text{C}_{14}$  trans,  $\text{C}_{15}=\text{N}$  syn configuration of retinal. The relationships of the retinal structures in the 13-demethyl pigment and its 150-ps intermediate to those in BR-548, BR-570, and their respective bathochromic intermediates in the native photocycle are discussed.

#### Introduction

Bacteriorhodopsin (BR) in *Halobacterium halobium* converts the energy of incident light into a proton gradient across the cell membrane and thereby permits bacterial growth under anaerobic conditions.<sup>1</sup> This biological function of BR as a light-driven proton pump is based, at least in part, on configurational and conformational changes in its retinal chromophore which is covalently bound to the protein through a protonated Schiff base. The

transmembrane proton gradient appears during a BR photocycle which usually is described in terms of structural and protonation changes in retinal<sup>2-5</sup> but which also involves analogous changes in the surrounding protein environment.

(1) For a comprehensive review see: Stoeckenius, W.; Bogomolni, R. A. *Annu. Rev. Biochem.* **1982**, *51*, 587-616.

(2) Lewis, A.; Spoonhower, J.; Bogomolni, R. A.; Lozier, R. H.; Stoeckenius, W. *Proc. Natl. Acad. Sci. USA* **1974**, *71*, 4462-4466.

(3) Stockburger, M.; Klusmann, W.; Gattermann, H.; Massig, G.; Peters, R. *Biochemistry* **1979**, *18*, 4886-4900.

(4) Aton, B.; Doukas, A. G.; Callender, R. H.; Becher, B.; Ebrey, T. G. *Biochemistry* **1977**, *16*, 2995-2999.

(5) Tsuda, M.; Glaccum, M.; Nelson, B.; Ebrey, T. G. *Nature (London)* **1980**, *287*, 351-353.

\* Authors to whom correspondence should be addressed.

<sup>†</sup> University of Arizona.

<sup>‡</sup> University of Freiburg.

<sup>§</sup> Senior Alexander von Humboldt Awardee.

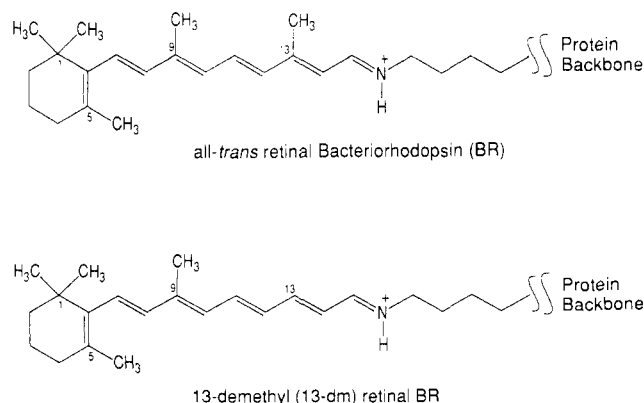


**Figure 1.** (Top) Chemical structure of retinal and Schiff base attachment to protein. Retinal configuration in solution and in crystalline forms is 6-s-cis while retinal is 6-s-trans in native bacteriorhodopsin (BR). (Bottom) Analogous 6-s-cis configuration of 13-demethylretinal in an artificial 13-dm BR pigment. The precise retinal configuration in 13-dm BR remains to be determined.

The initial BR sample can exist in two forms, light-adapted (LA) or dark-adapted (DA), depending upon the illumination conditions. The BR<sub>LA</sub> sample contains almost exclusively the all-trans isomer of retinal while the BR<sub>DA</sub> sample contains a nearly equal mixture of 13-cis and all-trans isomers. Both isomeric forms of retinal in BR undergo separate photocycles with durations of several milliseconds. The proton translocation activity, however, is only mediated by the all-trans isomer.<sup>6</sup>

Whereas the general biological function of BR is well understood, the molecular mechanisms describing the formation of specific intermediates during the BR<sub>LA</sub> and BR<sub>DA</sub> photocycles remain unresolved. Of particular importance is the mechanism by which the 13-cis and all-trans isomers of retinal are formed during the BR<sub>LA</sub> and BR<sub>DA</sub> photocycles.

Resonance Raman (RR) spectroscopy has proven to be a powerful method for measuring the vibrational structure of retinal in BR pigments and the changes that occur in retinal during the photocycle.<sup>7,8</sup> Given the complexity of the retinal RR spectrum, the selective variation of the retinal chemical structure and/or incorporation of isotopes is an important part of a detailed analysis. Several studies involving such isotopically substituted retinals have been completed, but these focus almost exclusively on the all-trans (BR<sub>LA</sub>) sample and its photocycle. Little information is available on the structural changes of retinal in the cis cycle. These latter studies are experimentally difficult since (i) maximally only half of the BR<sub>DA</sub> sample is 13-cis-retinal and (ii) the cis cycle re-forms the 13-cis isomer with only a moderate yield (i.e., optical excitation of the 13-cis isomer results in partial conversion to all-trans-retinal through light adaptation).

Recently, it has been shown that changes in the chemical structure of retinal can alter the cis/trans equilibrium even under light-adapted conditions.<sup>9-11</sup> The associated photocycles also change.<sup>12,13</sup> Different substitutions especially at the C<sub>13</sub> position have large effects.<sup>9</sup> For example, the 13-demethylretinal BR (13-dm-retinal BR) pigment (Figure 1) adopts primarily the 13-cis configuration ( $\approx 85\%$ ) under light-adapted conditions<sup>9</sup> and, therefore, is well suited for study of the photochemistry of the cis cycle. Artificial BR pigments prepared with structurally and/or isotopically modified retinals have been shown to be valuable not only in examining the native BR photocycle<sup>12,13</sup> but also in the

preparation of new photochromic materials which have potentially useful properties themselves.<sup>12,13</sup> The photocycles of artificial BR pigments have been examined only by transient absorption spectroscopy. Structure-sensitive spectroscopies, such as vibrational Raman scattering, have not been used to study the configurational and conformational changes occurring in the modified retinal chromophores during each artificial pigment photocycle.

RR spectra of the 13-dm pigments are presented in this paper together with the RR spectra of a bathochromic intermediate. Picosecond laser excitation between 532 and 590 nm is used to record RR spectra of the ground-state 13-dm BR pigment under low-energy conditions in order to minimize photochemistry. Deuterium shifts measured from H<sub>2</sub>O and D<sub>2</sub>O samples are used to make some vibrational mode assignments for retinal. These vibrational spectra suggest a C<sub>13</sub>=C<sub>14</sub> cis, C<sub>15</sub>=N syn configuration for the retinal chromophore in the 13-dm BR pigment. Picosecond time-resolved resonance Raman (PTR<sup>3</sup>) spectroscopy is used to record the RR spectrum of a bathochromic intermediate present 150 ps after the photocycle begins in both H<sub>2</sub>O and D<sub>2</sub>O solutions. The deuterium shifts in these PTR<sup>3</sup> data suggest that the 150-ps intermediate contains retinal in a C<sub>13</sub>=C<sub>14</sub> trans, C<sub>15</sub>=N syn configuration. The configurational changes in the photocycle of the 13-dm BR pigment also are discussed in terms of native BR photocycle.

## Experimental Section

**Materials and Methods.** *Halobacterium halobium* is grown in 12-L batch cultures following published procedures.<sup>14</sup> The purple membranes containing BR are isolated from the bacteria by using procedures described in ref 15. The native retinal is chemically released from the bacterioopsin apoprotein by using NH<sub>2</sub>OH and light. Specifically,  $1.25 \times 10^{-6}$  mol of native BR, as contained in the membrane patches, is suspended in a solution of 2.0 M NH<sub>2</sub>OH and 4.0 M NaCl (pH = 6.8 and 100 mL total volume). This solution is exposed to the filtered (500–900 nm) output of a 500-W projection bulb for 12 h which results in the complete detachment of the retinal from the bacterioopsin to form retinal oxime. The NH<sub>2</sub>OH and NaCl salts are removed by rapid dialysis. Bovine serum albumin (BSA from Sigma Chemical Co., A-6793) is added (1% w/v) to assist in the removal of the retinal oxime. The oxime is removed by repeated treatments with BSA until the sample absorbance at 380 nm (retinal oxime) is reduced to the level of the base-line scattering recorded for the membrane patches containing bacterioopsin.<sup>16</sup>

The artificial BR pigment is prepared by reconstituting 13-dm retinal, prepared and purified according to methods described elsewhere,<sup>9</sup> with bacterioopsin. The 13-dm-retinal ( $5.5 \times 10^{-6}$  mol in 0.1 mL of ethanol) is added to 30 mL (OD<sub>280</sub> = 10) of the membrane patches containing bacterioopsin and stirred for 16 h without exposure to light. The reconstitution of the 13-dm-retinal is monitored by the absorbance ratio,  $A_{560}/A_{280}$ , and is considered complete when this ratio becomes constant. The remaining unbound 13-dm-retinal is removed by ultrafiltration and the membranes are washed with distilled water. The membranes containing 13-dm-retinal are concentrated by ultrafiltration to have an OD<sub>560</sub> = 3.5–4.0. The exchangeable protons on both 13-dm retinal and the bacterioopsin are replaced with deuterons by diluting the protonated 13-dm-retinal membranes in 99.8% D<sub>2</sub>O (1:9). The deuterated sample is collected by ultrafiltration. This procedure is repeated twice to yield a >99% deuterated sample.

**Instrumentation.** The instrumentation used to record RR scattering from both ground-state 13-dm BR and from the 150-ps

(6) Fahr, A.; Bamberg, E. *FEBS Lett.* **1982**, *140*, 251–253.

(7) Smith, S. O.; Lugtenberg, J.; Mathies, R. A. *J. Membr. Biology* **1985**, *85*, 95–109.

(8) Stockburger, M.; Alshuth, T.; Oesterheld, D.; Gärtner, W. In *Spectroscopy of Biological Systems*; Clark, R. J. H., Hester, R. E., Eds.; Wiley: New York, 1986; pp 483–535.

(9) Gärtner, W.; Townner, P.; Hopf, H.; Oesterheld, D. *Biochemistry* **1983**, *22*, 2637–2644.

(10) Gärtner, W.; Oesterheld, D.; Vogel, J.; Maurer, R.; Schneider, S. *Biochemistry* **1988**, *27*, 3497–3502.

(11) Gärtner, W.; Oesterheld, D. *Eur. J. Biochem.* **1988**, *176*, 641–648.

(12) Sheves, M.; Ottolenghi, M. Molecular Mechanism for the Function of Bacteriorhodopsin and Visual Pigments: Studies with Model Compounds and Artificial Pigments. In *Chemistry and Biology of Synthetic Retinoids*; SRI International, Menlo Park, CA 1989 (in press).

(13) Ottolenghi, M.; Sheves, M. *J. Membr. Biol.*, in press.

(14) Oesterheld, D.; Stoeckenius, W. *Methods Enzymol.* **1976**, *31*, 667–678.

(15) Atkinson, G. H.; Blanchard, D.; Lemaire, H.; Brack, T. L.; Hayashi, H. *Biophys. J.* **1989**, *55*, 263–274.

(16) Hiraki, K.; Hamanaka, T.; Yoshihara, K.; Kito, Y. *Biochim. Biophys. Acta* **1987**, *891*, 177–193.

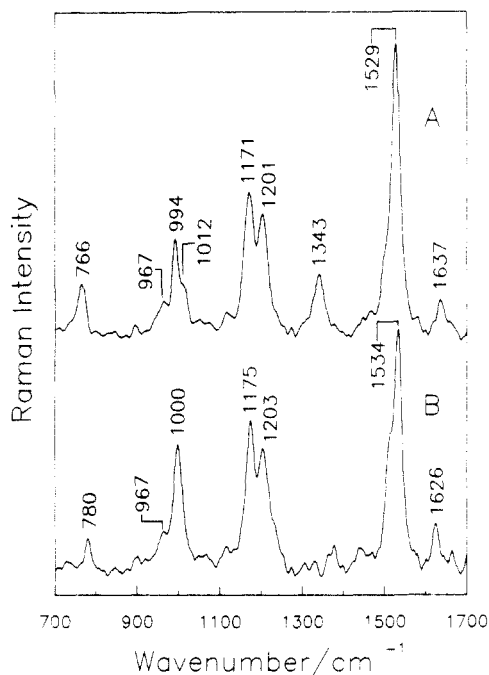


**Figure 2.** Low (600 grooves/mm grating) resolution resonance Raman (RR) spectra measured with the 582-nm dye laser excitation of 13-dm BR in (A)  $\text{H}_2\text{O}$  and (B)  $\text{D}_2\text{O}$ . The laser power is low enough (0.5 mW) to ensure that only RR scattering from the ground state of 13-dm BR is observed.

intermediate has been discussed in detail elsewhere,<sup>17</sup> and therefore only a brief description is given here. The fundamental output of a mode-locked Nd:YAG laser (Quantronix, Model 416) is frequency doubled in order to simultaneously excite two synchronously pumped dye lasers (Coherent, Model 702.3). Rhodamine 6G dye solutions are used to produce both the pump (568 nm) and probe (582 nm) laser outputs at repetition rates of 1 MHz. A temporal delay is introduced between the two dye laser pulses by diverting the probe laser pulse through an optical delay line. The two dye laser beams are made collinear before being focused by a microscope objective into the sample. The BR sample is used as a rapidly flowing (20 m/s) liquid jet which replaces the volume exposed to excitation between pairs of pump-probe laser pulses. RR scattering is collected perpendicular to the plane formed by the two dye laser beams and the liquid sample jet. The RR scattering is focused onto the slit of a 0.75-m triple monochromator (Spex Triplemate) the dispersion stage of which is equipped with either 600 or 1800 groove/mm gratings. An intensified diode array (EG&G, Model 1421) is used to detect the dispersed RR scattering.

## Results

**RR Spectrum of Ground-State 13-dm BR.** The RR spectra of the ground-state 13-dm-retinal BR pigment measured with 582-nm (6 ps pulse width, fwhm) excitation are presented in Figure 2 for two solvents,  $\text{H}_2\text{O}$  (A) and  $\text{D}_2\text{O}$  (B). The laser power is low enough (0.5 mW) to minimize photochemistry and, therefore, only RR scattering from the parent 13-dm chromophore is recorded. This same RR spectrum also is measured by using low-power (1 mW) picosecond laser excitation at 532 nm (70 ps fwhm), 570 nm (6 ps fwhm), and 590 nm (6 ps fwhm). All four RR spectra are the same as the 582-nm spectrum with respect to the frequency positions and relative intensities of the features and, therefore, no significant dependence on the excitation wavelength (532–590 nm) is observed.

The 1637- $\text{cm}^{-1}$  band is assigned to the Schiff base,  $\text{C}_{15}=\text{NH}^+$  stretching vibration due to the 11- $\text{cm}^{-1}$  decrease to 1626  $\text{cm}^{-1}$  in the ND derivative (Figure 2). The largest RR band, assignable

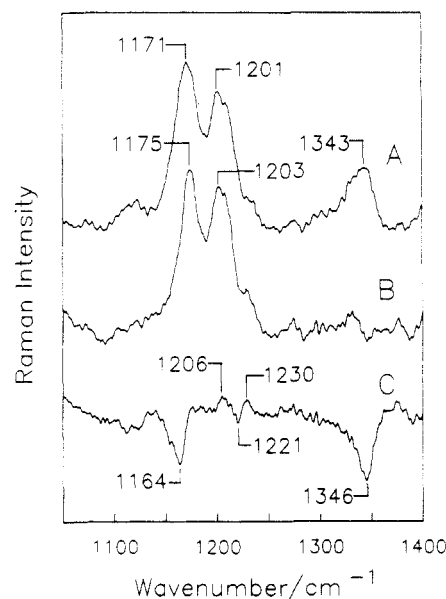


**Figure 3.** High (1800 grooves/mm grating) resolution resonance Raman spectra in the 1050–1400- $\text{cm}^{-1}$  region of 13-dm BR in (A)  $\text{H}_2\text{O}$  and (B)  $\text{D}_2\text{O}$ . The remaining experimental conditions are the same as in Figure 1. The difference signal (B - A) is shown in trace C.

to the  $\text{C}=\text{C}$  stretching modes, appears at 1529  $\text{cm}^{-1}$ . This displacement is near the 1527- $\text{cm}^{-1}$  position measured for BR-570<sup>18</sup> and is consistent with the small shift in the absorption maxima between 13-dm BR (565 nm)<sup>9</sup> and BR-570.

The large, single band at 1343  $\text{cm}^{-1}$  appears in a region associated with the C-H and N-H in-plane rocking modes. This band is assigned to the N-H in-plane rocking vibration due to the frequency decrease to a position near 1000  $\text{cm}^{-1}$  in  $\text{D}_2\text{O}$ <sup>19</sup> (Figure 2).

The fingerprint (C-C stretching mode) region near 1160–1210  $\text{cm}^{-1}$  contains information about the configuration of the retinylidene chromophore.<sup>18,19</sup> Two prominent bands appear at 1171 and 1201  $\text{cm}^{-1}$  in the  $\text{H}_2\text{O}$  sample and at 1175 and 1203  $\text{cm}^{-1}$  in the  $\text{D}_2\text{O}$  sample (Figure 3). RR spectra from this region are measured with a high-resolution grating (1800 grooves/mm) in order to expose the small changes that occur upon deuteration. These data are presented in Figure 3 for  $\text{H}_2\text{O}$  (A) and  $\text{D}_2\text{O}$  (B) solutions together with the difference (B - A) spectrum (Figure 3C). A large negative peak at 1164  $\text{cm}^{-1}$  implies that a band is hidden under the strong 1171- $\text{cm}^{-1}$  band and is shifted in  $\text{D}_2\text{O}$ . A small negative peak at 1221  $\text{cm}^{-1}$  and small positive peaks at 1206 and 1230  $\text{cm}^{-1}$  suggest that band changes also occur in this region. The negative peak at 1346  $\text{cm}^{-1}$  reflects the disappearance of the N-H in-plane rocking band upon deuteration vide supra.

The contributions to RR scattering from the  $\text{C}-\text{CH}_3$  in-plane rocking modes are significantly altered in 13-dm BR since the  $\text{C}_{13}-\text{CH}_3$  bond is replaced with a  $\text{C}_{13}-\text{H}$  bond. The RR intensity observed in this region arises from the remaining  $\text{C}-\text{CH}_3$  vibrations. This reduction in the number of in-plane  $\text{C}-\text{CH}_3$  modes in 13-dm BR is reflected in the small RR intensity at 1012  $\text{cm}^{-1}$  (Figure 2).

The hydrogen out-of-plane (HOOP) modes in 13-dm BR also are assigned to RR bands which undergo changes upon deuteration. Two intense bands appear at 994 and 766  $\text{cm}^{-1}$  while a weak shoulder can be found at 967  $\text{cm}^{-1}$ . Normal-mode calculations for 13-dm retinal assign the 994- $\text{cm}^{-1}$  band to the  $\text{C}_{15}\text{H}$  HOOP vibration.<sup>20</sup> From this assignment, a small decrease in the frequency position of the band is expected in  $\text{D}_2\text{O}$  because

(18) Smith, S. O.; Braiman, M. S.; Myers, A. B.; Pardo, J. A.; Courtin, J. M. L.; Winkel, C.; Lugtenburg, J.; Mathies, R. A. *J. Am. Chem. Soc.* **1987**, *109*, 3108–3125.

(19) Smith, S. O.; Pardo, J. A.; Lugtenburg, J.; Mathies, R. A. *J. Phys. Chem.* **1987**, *91*, 804–819.

(20) Curry, B.; Brock, A.; Lugtenburg, J.; Mathies, R. A. *J. Am. Chem. Soc.* **1982**, *104*, 5274–5286.

(17) Atkinson, G. H.; Brack, T. L.; Blanchard, D.; Rumbles, G. *Chem. Phys.* **1989**, *131*, 1–15.

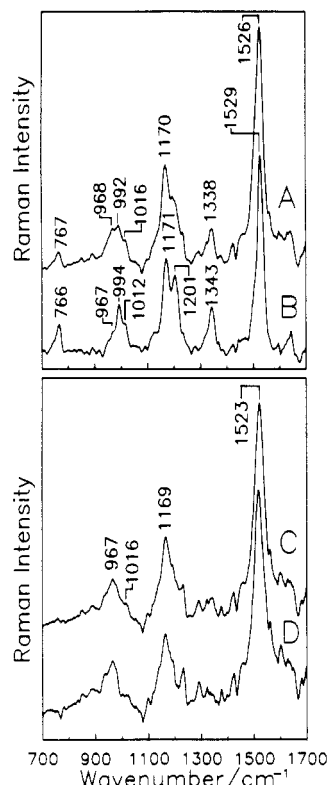


**Figure 4.** Low-resolution resonance Raman spectra of 13-dm BR in  $\text{H}_2\text{O}$  measured with (A) high-power (15 mW) and (B) low-power (0.5 mW) 582-nm excitation from a single laser. The difference signals (B -  $\theta$ A) obtained with scaling factors,  $\theta$ , of 0.7 and 0.5, respectively, are presented in traces C and D.

of the weak coupling with the N-H wagging mode. Unfortunately, the simultaneous decrease in the position of the N-D in-plane rocking band to about  $1000\text{ cm}^{-1}$  makes this assignment uncertain. The  $994\text{-cm}^{-1}$  band does not appear as a large feature in the RR spectrum of either the native BR-570 or BR-548.<sup>18,19</sup> The weak,  $967\text{-cm}^{-1}$  band can be assigned to the  $\text{HC}_7=\text{C}_8\text{H}$  and/or  $\text{H-C}_{11}=\text{C}_{12}\text{H}$  HOOP mode(s) while the intense  $766\text{-cm}^{-1}$  band can be assigned to the  $\text{HC}_{13}=\text{C}_{14}\text{H}$  HOOP mode.<sup>20</sup> This last band shifts to  $780\text{ cm}^{-1}$  in  $\text{D}_2\text{O}$  which suggests that this mode is coupled with the N-H wagging vibration. The relatively high intensity of the low-frequency HOOP band at  $766\text{ cm}^{-1}$  is similar to bands found in both BR-548 ( $800\text{ cm}^{-1}$ )<sup>19</sup> and low-temperature (77 K) K-630 ( $811\text{ cm}^{-1}$ ) in the native BR photocycle.<sup>21</sup>

**High-Power, Single Laser RR Data.** The RR spectrum of 13-dm BR measured with high-power (15 mW), 582-nm laser excitation (7 ps) is presented in Figure 4. A comparison of the high-power spectrum with that measured with low-power (0.5 mW) laser excitation reveals significant differences (Figure 4B). These spectral differences can be attributed to the formation of a photocycle intermediate during the high-power excitation pulse. The RR spectrum of the intermediate alone can be obtained by subtracting the low-power spectrum (13-dm BR only) from the high-power spectrum. Since the relative concentrations of the 13-dm BR ground state and the intermediate are not independently determined, the precise subtraction factor is unknown. Using the native BR photocycle as a guideline,<sup>17</sup> however, values between 0.7 and 0.4 can be used as an approximation (Figure 4). The features in the resultant difference spectra are almost independent of the subtraction factors over the 0.7–0.4 range: (i) the C=C stretching frequency decreases from  $1529\text{ cm}^{-1}$  (4B) to  $1523\text{ cm}^{-1}$  (4C), (ii) only one prominent RR band appears in the C-C stretching region (4C and 4D), and (iii) a strong HOOP wagging band appears at  $967\text{ cm}^{-1}$  (4C and 4D). A more detailed view of the features in the fingerprint and C-H and N-H in-plane

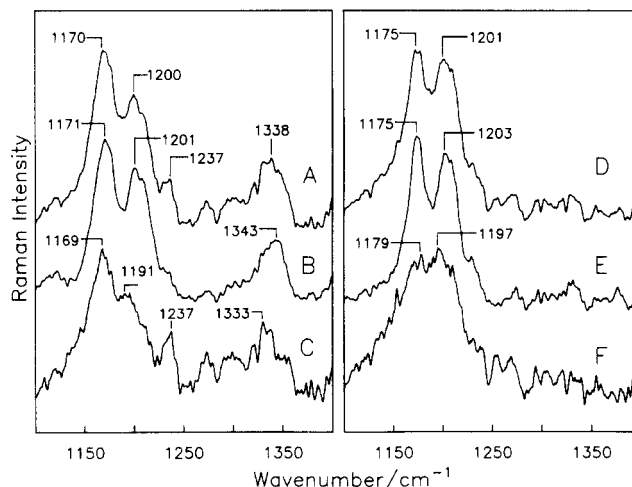


**Figure 5.** High-resolution resonance Raman (RR) spectra in the  $1100\text{--}1400\text{-cm}^{-1}$  region of 13-dm BR in (A, B, and C)  $\text{H}_2\text{O}$  and (D, E, and F)  $\text{D}_2\text{O}$ . RR spectra are measured at 582 nm (A and D) with 15 mW and (B and E) with 0.5 mW. The subtractions (A -  $\theta$ B) and (D -  $\theta$ E) shown respectively in C and F are performed with a scaling factor,  $\theta$ , of 0.6.

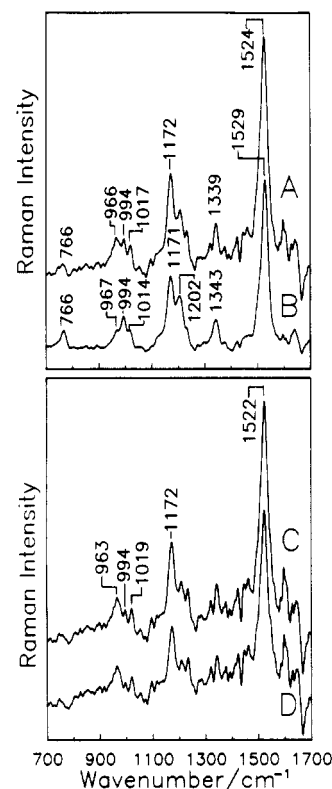


**Figure 6.** Picosecond time-resolved resonance Raman (PTR<sup>3</sup>) spectra of 13-dm BR and its photocycle intermediate K in  $\text{H}_2\text{O}$ . PTR<sup>3</sup> spectra are recorded at low resolution (600 grooves/mm grating) and with 10 mW of pump laser power at 568 nm and 2 mW of probe laser power at 582 nm. (A) PTR<sup>3</sup> spectrum with the probe laser pulse delayed by 150 ps relative to the pump laser pulse. (B) Probe laser only RR spectrum. (C) Difference signals (A -  $\theta$ B) obtained with  $\theta = 0.7$ . (D) Difference signal (A -  $\theta$ B) obtained with  $\theta = 0.5$ .

rocking regions can be obtained by using a higher resolution measurement. These spectra are presented in Figure 5 for both  $\text{H}_2\text{O}$  and  $\text{D}_2\text{O}$  solutions. The RR spectrum of the intermediate, obtained with a scaling factor of 0.6, exhibits a relatively intense band at  $1333\text{ cm}^{-1}$  for the  $\text{H}_2\text{O}$  sample (5C). This band disappears in the  $\text{D}_2\text{O}$  sample (Figure 5F), indicating that it can be assigned to the N-H in-plane rocking mode. In the C-C stretch region, three bands are observed at  $1169$ ,  $1191$ , and  $1237\text{ cm}^{-1}$ . In  $\text{D}_2\text{O}$  samples, the prominent  $1169\text{-cm}^{-1}$  band dramatically disappears and the C-C band shape transforms into a broad, featureless band with a maximum near  $1197\text{ cm}^{-1}$ .

(21) Braiman, M.; Mathies, R. A. *Proc. Natl. Acad. Sci. USA* **1982**, *79*, 403–407.

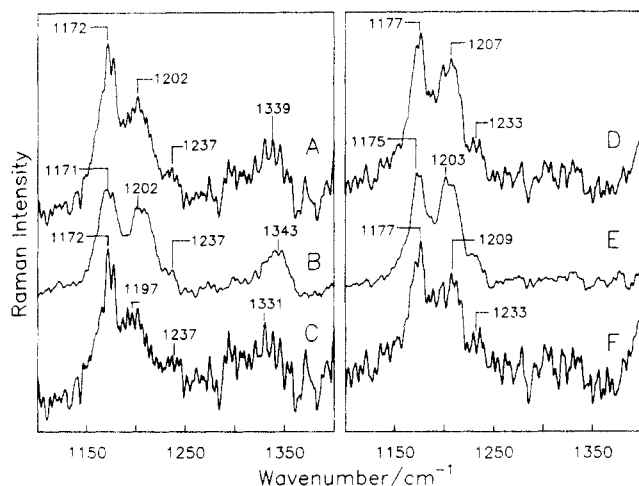


**Figure 7.** High-resolution PTR<sup>3</sup> spectra in the 1100–1400-cm<sup>-1</sup> region of 13-dm BR in (A, B, and C) H<sub>2</sub>O and (D, E, and F) D<sub>2</sub>O. The experimental conditions are the same as in Figure 5. (A and D) PTR<sup>3</sup> spectra with 150-ps time delay. (B and E) probe laser only spectra. (C and F) Difference signals (i.e., (A - 0B) and (D - 0E) with  $\theta = 0.6$ ).

**Picosecond, Time-Resolved RR Data.** PTR<sup>3</sup> spectra are measured with a 568-nm pump laser (10 mW) and a 582-nm probe laser (2 mW) delayed by 150 ps. These PTR<sup>3</sup> data are compared with the probe laser only spectra (2 mW) in Figure 6. The probe laser only spectrum measured with 2-mW excitation is basically the same as the spectrum measured with 0.5 mW (Figure 4B) except that a slightly larger HOOP band at 966 cm<sup>-1</sup> is observed in the 2-mW data. To obtain a spectrum of the photocycle intermediate at 150 ps, a difference RR spectrum is calculated (PTR<sup>3</sup> at 150 ps minus 2 mW probe laser only) in analogy to the analysis of the single laser experiment (i.e., Figure 4). The RR features in this difference spectrum also are not strongly dependent on the scaling factor used in the 0.7–0.4 range and are similar to those observed in the high-power, single-laser experiment (Figure 4). Specifically, the frequency of the C=C stretching mode decreases to 1522 cm<sup>-1</sup>, and in the C-C stretching region, only one prominent band appears. In the HOOP region, the 963-cm<sup>-1</sup> band remains strong, but with less intensity than in the spectrum measured by the high-power, single-laser excitation (Figure 4). Another HOOP band at 994 cm<sup>-1</sup> also is resolved in this PTR<sup>3</sup> spectrum.

High-resolution spectra of the C-C stretching and C-H and N-H in-plane rocking regions measured in both H<sub>2</sub>O and D<sub>2</sub>O are presented in Figure 7. The corresponding difference spectra are calculated with a subtraction factor of 0.6. The relatively strong band near 1330 cm<sup>-1</sup> observed in the H<sub>2</sub>O sample disappears completely in a D<sub>2</sub>O solution (Figure 7), suggesting that this band be assigned to the N-H in-plane rocking mode. The band shapes in the fingerprint region also are different than those in the single-laser RR spectrum (Figure 5). The prominent band near 1170 cm<sup>-1</sup> in the PTR<sup>3</sup> spectrum is sharper and has a higher frequency (1172 cm<sup>-1</sup>) than in the single-laser data (1169 cm<sup>-1</sup>). In the D<sub>2</sub>O sample, the intensity of the 1172-cm<sup>-1</sup> band also decreases and a new shoulder appears near 1209 cm<sup>-1</sup>.

## Discussion

**Ground-State 13-dm BR.** The configuration and conformation of the retinal chromophore in the ground state of 13-dm BR can be characterized from the RR spectra presented here for low-power laser excitation (Figures 2 and 3). This analysis is based on RR studies of isotopically substituted retinals examined both in solution<sup>20,22,23</sup> and in the BR membrane.<sup>18,19</sup>

The intense RR band observed at 1343 cm<sup>-1</sup> (Figures 2 and 3) can be assigned to an N-H in-plane rocking mode. When

C<sub>15</sub>=N is in a syn configuration, this N-H mode strongly couples with a C<sub>15</sub>-H in-plane rocking mode to form an antisymmetric combination mode which appears with high intensity.<sup>19</sup> Based on these assignments, the observation of an intense N-H rocking band at 1343 cm<sup>-1</sup> suggests that the C<sub>15</sub>=N configuration in 13-dm BR is syn.

The C<sub>14</sub>-C<sub>15</sub> stretching vibration has been described as a marker band characterizing the C<sub>13</sub>=C<sub>14</sub> and C<sub>15</sub>=N configurations.<sup>19,24</sup> For the syn configuration of C<sub>15</sub>=N, the C<sub>14</sub>-C<sub>15</sub> stretching mode is strongly coupled with the N-H rocking mode while for the anti C<sub>15</sub>=N configuration, no coupling occurs. These relationships were established from measurements of both deuterium shifts and absolute frequency positions of native BR.<sup>19,24</sup> For example, the RR spectrum of BR-548 (C<sub>15</sub>=N syn) exhibits an increase in the C<sub>14</sub>-C<sub>15</sub> frequency from 1167 to 1201 cm<sup>-1</sup> when the solvent is changed from H<sub>2</sub>O to D<sub>2</sub>O while no change is observed in the BR-570 (C<sub>15</sub>=N anti) spectra.<sup>18,19</sup> The degree of coupling between the C<sub>14</sub>-C<sub>15</sub> stretching vibration and the N-H rock, therefore, can be used to determine the C<sub>15</sub>=N configuration. In addition, the absolute frequency position of the C<sub>14</sub>-C<sub>15</sub> band is sensitive to the C<sub>13</sub>=C<sub>14</sub> and C<sub>15</sub>=N configuration. Calculations indicate that the C<sub>14</sub>-C<sub>15</sub> frequency decreases by  $\approx 10$  cm<sup>-1</sup> when a cis C<sub>13</sub>=C<sub>14</sub> is present and by  $\approx 20$  cm<sup>-1</sup> when C<sub>15</sub>=N has a syn configuration.<sup>19</sup>

The spectral changes induced by N-H deuteration in 13-dm BR are evident in the difference spectrum presented in Figure 3C. The disappearance of the RR band at 1164 cm<sup>-1</sup> upon deuteration (negative band, Figure 3C) reflects the strong coupling with the N-H rocking mode that is consistent with the C<sub>14</sub>-C<sub>15</sub> assignment of the 1164-cm<sup>-1</sup> band. Based on previous studies,<sup>18,19</sup> these data indicate that the C<sub>15</sub>=N configuration in 13-dm BR is syn. The assignment of a syn configuration is supported by the appearance of small positive bands at 1206 and 1230 cm<sup>-1</sup> in Figure 3C. Both are likely candidates for the shifted position of the 1164-cm<sup>-1</sup> band caused by deuteration with preference given to the 1206-cm<sup>-1</sup> band since such a shift correlates well with that observed in BR-548 (i.e., 1167 to 1201 cm<sup>-1</sup>).<sup>19</sup> With regard to the absolute frequency position, the low 1164-cm<sup>-1</sup> frequency of the C<sub>14</sub>-C<sub>15</sub> stretch, which is comparable to the 1167-cm<sup>-1</sup> band in BR-548,<sup>19</sup> indicates that the C<sub>13</sub>=C<sub>14</sub> configuration is cis.

The intense 766-cm<sup>-1</sup> HOOP band (Figure 2) is similar to the results obtained from BR-548 where the intense C<sub>14</sub>-H HOOP band appears at 800 cm<sup>-1</sup>. The decrease in the frequency of the C<sub>14</sub>-H HOOP mode from 800 to 766 cm<sup>-1</sup> for 13-dm BR may be caused by the coupling between the C<sub>14</sub>-H and C<sub>13</sub>-H HOOP modes.<sup>20</sup> The high intensity of the 766-cm<sup>-1</sup> band suggests that the polyene is twisted near the C<sub>14</sub> or C<sub>13</sub> positions of the retinal chromophore.

In summary, the C<sub>13</sub>=C<sub>14</sub> cis, C<sub>15</sub>=N syn configuration of the retinal chromophore in the ground state of 13-dm BR is very similar to that of BR-548, in spite of the absence of the CH<sub>3</sub> substituent at the C<sub>13</sub> position. The 13-dm BR configuration also is consistent with the results of chromophore extraction experiments which demonstrated that >85% of the 13-dm pigment has a 13-cis configuration.<sup>9</sup> There are, however, some clear differences between 13-dm BR and BR-548 RR spectra. The strong HOOP band at 994 cm<sup>-1</sup> is not observed from BR-548. This band is tentatively assigned to the C<sub>15</sub>H wagging mode in accordance with normal-mode calculations for 13-dm-retinal.<sup>20</sup> The high intensity of this band may arise from out-of-plane distortion near the Schiff base position. This means that the absence of the CH<sub>3</sub> group at the C<sub>13</sub> position changes the interaction between retinal and its protein environment near the Schiff base part of the chromophore. The red shift of the absorption maximum of 13-dm BR compared with that of the BR-548 (565 to 548 nm) also is attributable to such a structural difference.

Previously, the RR spectrum of the 13-dm BR at a low (80 K) temperature has been reported.<sup>25</sup> While most of the RR band

(22) Curry, B.; Palings, I.; Broek, A.; Pardo, J. A.; Mulder, P. J. J.; Lugtenburg, J.; Mathies, R. A. *J. Phys. Chem.* **1984**, *88*, 688–702.

(23) Smith, S. O.; Myers, A. B.; Mathies, R. A.; Pardo, J. A.; Winkel, L.; van den Berg, E. M. M.; Lugtenburg, J. *Biophys. J.* **1985**, *47*, 653–664.

(24) Smith, S. O.; Myers, A. B.; Pardo, J. A.; Winkel, C.; Mulder, P. J. J.; Lugtenburg, J.; Mathies, R. A. *Proc. Natl. Acad. Sci. USA* **1984**, *81*, 2055–2059.

frequencies correspond to within  $\pm 5\text{ cm}^{-1}$  of the data presented here, several bands appear at significantly different positions (e.g., 1022 and  $1332\text{ cm}^{-1}$ <sup>25</sup> instead of 1012 and  $1343\text{ cm}^{-1}$ , respectively). Furthermore, the relative intensities of bands differ. In the 80 K spectrum, the  $1205\text{-cm}^{-1}$  band is much smaller than the  $1175\text{-cm}^{-1}$  band in the C–C stretching region, and the  $994\text{-cm}^{-1}$  HOOP band is relatively small compared with the  $1022\text{-cm}^{-1}$  C–CH<sub>3</sub> rocking band.<sup>25</sup> These differences cannot be attributed directly to changes in the excitation wavelengths since the 520.8-nm laser excitation used previously is close to the 532-nm excitation used here. It is more likely that the different RR spectra, especially the smaller intensity of the  $994\text{-cm}^{-1}$  band, reflect different chromophoric structures at the two temperatures. This same type of observation has been reported from PTR<sup>3</sup> studies of the K-590 intermediate of native BR.<sup>21,26–28</sup>

**Photocycle Intermediates.** The photocycle of 13-dm BR has been investigated by using time-resolved absorption spectroscopy with time resolutions ranging from  $10^{-12}$  to 1 s.<sup>10,29–31</sup> The formation of a K-like species having a red-shifted absorption maximum ( $>600\text{ nm}$ ) within 5 ns after excitation has been reported.<sup>29</sup> This bathochromic intermediate decays with a time constant of 250 ms.<sup>10</sup> Recently, "J" and "K" species have been reported to exist in the early stages of the 13-dm photocycle.<sup>30</sup> The time constant of the transition from the optically populated excited state to "J" and from "J" to "K" was reported to be 1.2 and 3 ps, respectively.<sup>30</sup> In this discussion, these J-like and K-like species in the 13-dm BR photocycle are designated J<sup>DM</sup> and K<sup>DM</sup>, respectively.

The high-power single-laser experiments utilize a 7-ps pulse width to both initiate the photocycle and generate RR scattering from the resultant reaction mixture. Based on the reported time constants,<sup>30</sup> both J<sup>DM</sup> and K<sup>DM</sup> should be present in the reaction mixture created and, therefore, the RR scattering should contain contributions from both transient species.<sup>32</sup> By contrast, the two-laser, pump-probe data reported here are recorded with a 150-ps delay which ensures that the only photochemical intermediate present is K<sup>DM</sup>. Since the reaction mixtures measured with RR scattering are different in these two cases, the resultant RR spectra of the intermediates also should differ. This is substantiated by the spectral differences observed in the C–C stretching and HOOP regions between the single-laser data and the PTR<sup>3</sup> results (Figures 4–7). Such comparisons are made, of course, after RR scattering from ground-state 13-dm has been removed.

Specifically, in comparison with the parent 13-dm BR, the C=C stretching frequency decreases by  $6\text{--}7\text{ cm}^{-1}$  in both the J<sup>DM</sup> + K<sup>DM</sup> spectrum (Figure 4B, cf. Figure 4C,D) and the K<sup>DM</sup> spectrum (Figure 6B, cf. Figure 6C,D). This decrease is consistent with the bathochromic shift of absorption maxima of these two species. The N–H in-plane rocking mode ( $1330\text{--}40\text{ cm}^{-1}$ ) has relatively strong intensities in both the spectra indicating that the J<sup>DM</sup> and K<sup>DM</sup> intermediates preserve the C<sub>15</sub>=N syn configuration.<sup>19</sup> These assignments are supported in the RR spectra recorded in a D<sub>2</sub>O solvent (Figures 5 and 7).

Differences in the C–C stretching region appear between the K<sup>DM</sup> RR spectra obtained in H<sub>2</sub>O and D<sub>2</sub>O. The band at  $1172\text{ cm}^{-1}$

$\text{cm}^{-1}$  increases upon deuteration and a new shoulder appears at  $1209\text{ cm}^{-1}$  (Figure 7, C and F). Such a frequency increase in D<sub>2</sub>O suggests that the C<sub>14</sub>–C<sub>15</sub> stretching mode coupled with N–H rocking mode is located at  $1172\text{ cm}^{-1}$ , in analogy with the C<sub>14</sub>–C<sub>15</sub> assignment of the parent chromophore. Since this type of coupling occurs for a C<sub>15</sub>=N syn configuration,<sup>19</sup> the frequency shift of the C<sub>14</sub>–C<sub>15</sub> stretching mode supports the assignment of a C<sub>15</sub>=N syn configuration to K<sup>DM</sup>.

In the RR spectra of ground-state 13-dm BR measured with a low-power laser, the C<sub>14</sub>–C<sub>15</sub> stretching mode appears as a negative band at  $1164\text{ cm}^{-1}$  in the difference signal (Figure 3C). Normal-mode calculations of the protonated Schiff base (PSB) retinal show that a  $10\text{-cm}^{-1}$  increase in the C<sub>14</sub>–C<sub>15</sub> stretching frequency occurs when the configuration is changed from the 13-cis to 13-trans.<sup>19</sup> The observed increase from  $1164$  to  $1172\text{ cm}^{-1}$  in K<sup>DM</sup>, therefore, suggests that this intermediate has a 13-trans configuration.

The frequency of the C<sub>14</sub>–C<sub>15</sub> stretching mode in the J<sup>DM</sup> + K<sup>DM</sup> mixture also may be used to characterize the configuration of J<sup>DM</sup> relative to that of K<sup>DM</sup>. The  $1169\text{-cm}^{-1}$  band which decreases in D<sub>2</sub>O can be assigned to the C<sub>14</sub>–C<sub>15</sub> stretching mode (Figure 5C). The C<sub>14</sub>–C<sub>15</sub> frequency in the mixture shifts by  $5\text{ cm}^{-1}$  from that recorded for the ground state of 13-dm BR ( $1164\text{ cm}^{-1}$ , Figure 3C) while it shifts by  $8\text{ cm}^{-1}$  in K<sup>DM</sup> ( $1172\text{ cm}^{-1}$ , Figure 7C). This  $3\text{-cm}^{-1}$  difference suggests that the retinal configuration near C<sub>13</sub>=C<sub>14</sub> in J<sup>DM</sup> differs from those of both K<sup>DM</sup> and ground-state 13-dm BR and, therefore, the configuration of J<sup>DM</sup> represents an intermediate structure formed during the transformation from 13-cis to all-trans.

In the HOOP region, an intense band at  $963\text{ cm}^{-1}$  appears in the K<sup>DM</sup> spectrum, indicating that this intermediate has a distorted (e.g., twisted) polyene chain and is not relaxed to a planar form. The J<sup>DM</sup> + K<sup>DM</sup> spectrum contains an even stronger  $967\text{-cm}^{-1}$  band (Figure 4), indicating that J<sup>DM</sup> is more distorted than K<sup>DM</sup>. This observation supports the view that J<sup>DM</sup> has a transient structure intermediate between 13-cis to all-trans.

This analysis demonstrates clearly that the K<sup>DM</sup> intermediate has a 13-trans, 15-syn configuration while the ground-state chromophore in 13-dm BR has a 13-cis, 15-syn configuration. It also suggests that J<sup>DM</sup> has a distinct structure which is formed during the transformation of the parent 13-dm chromophore into the K<sup>DM</sup> intermediate. In the photochemical process which converts 13-dm BR into K<sup>DM</sup>, isomerization occurs only at the C<sub>13</sub>=C<sub>14</sub> bond while the C<sub>15</sub>=N bond remains unchanged. This conclusion is consistent with a mechanism associated with the light-adapted photocycle of native BR in which photoisomerization occurs only at the C<sub>13</sub>=C<sub>14</sub> position. The photocycle of the 13-dm BR apparently emulates this mechanism by isomerizing at only one C=C bond in its bathochromic step.

Although the experimental difficulties mentioned earlier have limited studies of the dark-adapted, BR-548 photocycle, results do indicate that a bathochromic intermediate with a long ( $\approx 40\text{ ms}$ ) lifetime and an absorption maximum at about  $610\text{ nm}$  is formed.<sup>31,33–36</sup> The similarities of the bathochromic absorption, the long lifetime, and the vibrational structure of the parent retinal chromophore suggest that the K<sup>DM</sup> intermediate in the 13-dm BR photocycle corresponds to the bathochromic intermediate observed in the photocycle of BR-548. A recent FTIR study of native BR species trapped at low temperature concluded that the configuration of the K-like intermediate in the dark-adapted, cis cycle is 13-trans, 15-syn.<sup>37</sup> The analysis described here for the bathochromic intermediate in the 13-dm BR photocycle assigned the same retinal configuration. BR-548 (13-cis, 15-syn) is

(25) Schiffmiller, R.; Callender, R. H.; Waddell, W. H.; Govindjee, R.; Ebrey, T. G.; Kakitani, H.; Honig, B.; Nakanishi, K. *Photochem. Photobiol.* **1986**, *41*, 563–567.

(26) Terner, J.; Hsieh, C. L.; Burns, A. R.; El-Sayed, M. A. *Proc. Natl. Acad. Sci. USA* **1979**, *76*, 3046–3050.

(27) Smith, S. O.; Braiman, M.; Mathies, R. A. In *Time-Resolved Vibrational Spectroscopy*; Atkinson, G. H., Ed.; Academic Press: New York, 1983; pp 219–230.

(28) Brack, T. L.; Atkinson, G. H. *J. Mol. Struct.* **1989**, *214*, 289–303.

(29) Trissl, H.-W.; Gärtner, W. *Biochemistry* **1987**, *26*, 751–758.

(30) Zinth, W.; Dobler, J.; Franz, M. A.; Kaiser, W. In *Spectroscopy of Biological Molecules-New Advances*; Schmid, E. D., Schneider, F. W., Siebert, F., Eds.; Wiley: New York, 1988; pp 269–274.

(31) Hofrichter, J.; Henry, E. R.; Lozier, H. *Biophys. J.* **1989**, *56*, 693–706.

(32) Vibrationally excited ground-state 13-dm BR also may be formed during the 7-ps pulsed excitation, although independent data demonstrating its presence have not been reported and, therefore, it is not considered here.

(33) Sperling, W.; Carl, P.; Rafferty, C. N.; Dencher, N. A. *Biophys. Struct. Mechanism* **1977**, *3*, 79–94.

(34) Sperling, W.; Rafferty, C. N.; Kohl, K.-D.; Dencher, N. A. *FEBS Lett.* **1979**, *97*, 129–132.

(35) Kalisky, O.; Goldschmidt, C. R.; Ottolenghi, M. *Biophys. J.* **1977**, *19*, 185–189.

(36) Iwasa, T.; Tokunaga, F.; Yoshizawa, T. *Photochem. Photobiol.* **1981**, *33*, 539–545.

(37) Roepe, P. D.; Ahl, P. L.; Herzfeld, J.; Lugtenburg, J.; Rothschild, K. J. *J. Biol. Chem.* **1988**, *263*, 5110–5117.

thermally equilibrated with BR-570 (13-trans, 15-anti) by the double isomerization of the  $C_{13}=C_{14}$  and  $C_{15}=N$  bonds over a 20-min period. The BR-548 photocycle involves  $C_{13}=C_{14}$  isomerization to form a bathochromic species, K (13-trans, 15-syn). Thermally, the reverse isomerization occurs from the K to reform BR-548 with a time constant of  $\approx 40$  ms.

With respect to the light-induced conversion of BR-548 to BR-570, two mechanisms have been discussed.<sup>31,33-36</sup> In the first,<sup>31,33-36</sup> the bathochromic (K) intermediate after absorbing light decays directly to BR-570. In the second,<sup>35</sup> K converts into the K-610 intermediate of the trans photocycle (13-cis, 15-anti) after the absorption of light. Both processes, therefore, involve secondary photochemistry at the Schiff base. In the first mechanism, only a single isomerization at the  $C_{15}=N$  bond occurs, while in the second, a double isomerization at both the  $C_{13}=C_{14}$  and the  $C_{15}=N$  bonds is required. If the double isomerization of K to K-610 occurs with the same rate as the slow (20 min) double isomerization between BR-548 and BR-570,<sup>35</sup> then the  $K \rightarrow K-610$  quantum yield relative to that of dark-adapted, cis cycle can be estimated to be  $\Phi_K$  (40 ms/20 min)  $< 3 \times 10^{-5}$ , where  $\Phi_K$

( $< 1$ ) is the quantum yield for the formation of K. This calculated yield is much smaller than the proposed value of  $3 \times 10^{-2}$ ,<sup>35</sup> suggesting that such a double isomerization is not likely to be of importance in the light-induced transition from BR-548 to BR-570. From the data presented here, it is more likely that the K intermediate in the BR-548 photocycle is converted directly to BR-570 by the thermal isomerization of the  $C_{15}=N$  bond.

**Acknowledgment.** We thank T. Brack, D. Blanchard, and S. Ruskin for their technical assistance in these experiments. This work was supported by a grant (GM 36628-03) from the National Institutes of Health and by the DuPont Corp. through its funding of a Japanese-American exchange program between the University of Tokyo and the University of Arizona. W.G. expresses his gratitude to the Deutsche Forschungsgemeinschaft which supported a visit to the University of Arizona as part of this collaboration. G.H.A. gratefully acknowledges the support of the Alexander von Humboldt-Stiftung and the hospitality of Prof. E. Schlag at the Technical University of Munich where part of this paper was prepared.

## Time-Dependent Reaction Rates in the Thermolysis of a Poly(vinylnaphthalene endoperoxide)

M. R. Wixom

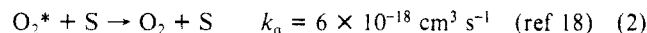
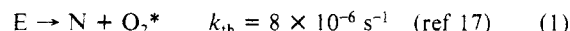
KMS Fusion, Inc., P.O. Box 1567, Ann Arbor, Michigan 48106-1567 (Received: October 19, 1989)

Classical reaction kinetics with time-independent rate constants have failed to provide a satisfactory explanation of the rate of thermolysis leading to the release of excited ( $^1\Delta_g$ ) molecular oxygen from polymer solutions and thin solid films of 1,4-dimethyl-2-poly(vinylnaphthalene 1,4-endoperoxide). First-order kinetics with time-dependent rates are shown to produce better agreement with the experimental data. The thermolysis rate constant is observed to have the time dependent  $k \sim t^{\alpha-1}$ , where  $\alpha = 0.66$  for polymer solutions and  $\alpha = 0.38$  for polymer thin films. The value of  $\alpha$  indicates the distribution of lifetimes for excited oxygen. The lifetime distribution is broadened by local concentration effects in the polymer.

### Introduction

Polymer-immobilized naphthalenes have been developed as chemical generators of singlet ( $^1\Delta_g$ ) oxygen.<sup>1-5</sup> The naphthalenes and other polynuclear aromatics can undergo transannular addition reactions with singlet oxygen to form 1,4-endoperoxides.<sup>6-10</sup> Subsequent thermolysis of these endoperoxides produces the original aromatic system and singlet oxygen.<sup>1,3,10-16</sup> Thus, aromatic systems that form stable endoperoxides can provide a clean and rapid source of singlet oxygen which can be used in synthetic chemical reactions or chemical laser pumping schemes.

Several previous studies have reported kinetic data for thermolysis reactions of aromatic hydrocarbon endoperoxides. Naphthalene derivatives are among the most extensively studied. The naphthalene derivatives have included 1,4-dimethylnaphthalene (DMN) in solution,<sup>3</sup> poly(1,4-dimethyl-2-vinylnaphthalene) (2PVN) in solution,<sup>3</sup> and 2PVN in thin films.<sup>2</sup> The thermolysis reactions of the endoperoxides (DMNE and 2PVNE) in solution were reported to follow simple first-order kinetics consistent with the following reaction scheme:



where E is the endoperoxide, N is the unoxidized naphthalene, and  $O_2^*$  is the excited singlet oxygen. The second reaction indicates a physical quenching mechanism where S is a solvent molecule. Since [S] is a constant  $\approx 10^{21} \text{ cm}^{-3}$  and  $k_q[S] \gg k_{th}$ , reaction 1 is the rate-limiting step.

The thermolysis reaction rate can be conveniently determined by using UV absorption spectrometry to follow the rise in naphthalene concentration. For room temperature measurements, the naphthalene peak at 290 nm is recorded over a period of several hours or days. The integrated rate law for reaction 1 can be expressed as a function of the naphthalene concentration [N]:

$$\ln \frac{[N]_t - [N]}{[N]_t - [N]_0} = -kt \quad (3)$$

(17) Twarowski, A. J. *Phys. Chem.* **1988**, 92, 6580.

(18) Monroe, B. M. In *Singlet O<sub>2</sub>*; Frimer, A. A., Ed.; CRC Press: Boca Raton, FL, 1985; p 177.

- (1) Saito, I.; Nagata, R.; Matsuura, T. *Tetrahedron Lett.* **1981**, 22(42), 4231.
- (2) Twarowski, A. J.; Good, L.; Busch, G. J. *Phys. Chem.* **1988**, 92, 396.
- (3) Saito, I.; Nagata, R.; Matsuura, T. *J. Am. Chem. Soc.* **1985**, 107, 6329.
- (4) Twarowski, A.; Dao, P. J. *Phys. Chem.* **1988**, 92, 5292.
- (5) McCall, D. B. Ph.D. Dissertation Part 2, Wayne State University, 1985.
- (6) Gollnick, K.; Schenck, G. O. In *1,4 Cycloaddition Reactions*; Hamer, J., Ed.; Academic: New York, 1967; p 255.
- (7) Rigaudy, J. *Pure Appl. Chem.* **1968**, 16, 169.
- (8) Denny, R. W.; Nickon, A. *Org. React.* **1973**, 20, 133.
- (9) Saito, I.; Matsuura, T. In *Singlet Oxygen*; Wasserman, H. H., Murray, R. W., Eds.; Academic: New York, 1971; p 511.
- (10) Bloodworth, A. J.; Eggelte, H. J. In *Singlet Oxygen*; Frimer, A. A., Ed.; CRC Press: Boca Raton, FL, 1985; Vol. II, p 93.
- (11) Murray, M. W. In *Singlet Oxygen*; Wasserman, H. H., Murray, R. W., Eds.; Academic: New York, 1979; p 59.
- (12) Wasserman, H. H.; Scheffer, J. R. *J. Am. Chem. Soc.* **1967**, 89, 3073.
- (13) Wasserman, H. H.; Larsen, D. L. *Chem. Commun.* **1972**, 253.
- (14) Larsen, D. L. Ph.D. Dissertation, Yale University, 1973.
- (15) Schaeffer-Ridder, M.; Brocker, U.; Vogel, E. *Angew. Chem.* **1976**, 88, 267.
- (16) Turro, N. J.; Chow, M. F.; Rigaudy, J. *J. Am. Chem. Soc.* **1981**, 103, 218.